

THO2, a core member of the THO/TREX complex, is required for microRNA production in Arabidopsis

Anchilie G. Francisco-Mangilet^{1,†,‡}, Patricia Karlsson^{2,†}, Myung-Hee Kim¹, Hyeon Ju Eo¹, Sung Aeong Oh¹, Jeong Hoe Kim³, Franceli Rodrigues Kulcheski^{2,§}, Soon Ki Park^{1,4,*} and Pablo Andrés Manavella^{5,*}

¹School of Applied Biosciences, Kyungpook National University, Daegu 702-701, Korea,

²Department of Molecular Biology, Max Planck Institute for Developmental Biology D-72076, Tübingen, Germany,

³Department of Biology, Kyungpook National University, Daegu 702-701, Korea,

⁴National Academy of Agricultural Science, Rural Development Administration, Jeonju 560-500, Korea, and

⁵Instituto de Agrobiotecnología del Litoral, Universidad Nacional del Litoral/CONICET, 3000 Santa Fe, Argentina

Received 14 April 2015; accepted 5 May 2015; published online 14 May 2015.

*For correspondence (e-mails psk@knu.ac.kr or pablomanavella@ial.santafe-conicet.gov.ar).

†These authors contributed equally to this work.

‡Present address: T.T. Chang Genetic Resources Center, International Rice Research Institute, 4031 Los Baños, Philippines.

§Present address: Centro de Biotecnologia da Universidade Federal do Rio Grande do Sul, Porto Alegre, Brazil.

SUMMARY

The THO/TREX complex mediates transport of nascent mRNAs from the nucleus towards the cytoplasm in animals, and has a role in small interfering RNA-dependent processes in plants. Here we describe five mutant alleles of *Arabidopsis thaliana* *THO2*, which encodes a core subunit of the plant THO/TREX complex. *tho2* mutants present strong developmental defects resembling those in plants compromised in microRNA (miRNA) activity. In agreement, not only were the levels of siRNAs reduced in *tho2* mutants, but also those of mature miRNAs. As a consequence, a feedback mechanism is triggered, increasing the amount of miRNA precursors, and finally causing accumulation of miRNA-targeted mRNAs. Yeast two-hybrid experiments and confocal microscopy showed that THO2 does not appear to interact with any of the known miRNA biogenesis components, but rather with the splicing machinery, implying an indirect role of THO2 in small RNA biogenesis. Using an RNA immunoprecipitation approach, we found that THO2 interacts with miRNA precursors, and that *tho2* mutants fail to recruit such precursors into the miRNA-processing complex, explaining the reduction in miRNA production in this mutant background. We also detected alterations in the splicing pattern of genes encoding serine/arginine-rich proteins in *tho2* mutants, supporting a previously unappreciated role of the THO/TREX complex in alternative splicing.

Keywords: *Arabidopsis thaliana*, gene silencing, micro RNA, small RNAs, THO2, THO/TREX complex.

INTRODUCTION

Among the mechanisms for post-transcriptional gene silencing in plants, small RNA-dependent gene regulation plays a central role (Baulcombe, 2004). MicroRNAs (miRNAs) are a specific class of small RNAs (mostly 21–22 nucleotides long) that mediate endogenous gene silencing (Jones-Rhoades *et al.*, 2006). In plants, DICER-LIKE1 (DCL1) processes mature miRNAs from long primary miRNA transcripts (pri-miRNAs) that form a stem-loop secondary structure. During processing in nuclear dicing bodies, DCL1 requires the assistance of the zinc finger protein SERRATE (SE) and the double-stranded RNA-binding protein HYPOASTIC LEAVES1 (HYL1) for accurate excision of the miRNAs (Fang and Spector, 2007; Fujioaka *et al.*, 2007; Voinnet, 2009). The mature miRNAs

associate with an ARGONAUTE (AGO) protein and guide the RNA-Induced Silencing Complex (RISC) Complex, through sequence complementarity, to their target mRNAs, ultimately silencing them. In contrast, production of small interfering RNAs (siRNAs), a different class of small RNAs, is based on processing of a highly complementary double-stranded RNA by a DCL1-independent pathway. In a very specialized pathway, *trans*-acting siRNAs (tasiRNAs) and secondary siRNAs are produced from *Trans-acting siRNA* (*TAS*) or even mRNA transcripts after initial cleavage by a miRNA (Chapman and Carrington, 2007). The production of tasiRNAs follows a particular process that shares components with both the miRNA and siRNA biogenesis pathways.

In yeast and animals, the THO/TREX complex has been characterized as a multimeric protein complex that mediates transcription elongation (yeast), splicing of mRNAs (animals), and export of mRNAs from the nucleus (both yeast and animals) (Reed and Cheng, 2005). In all studied organisms, the complex comprises TEX1 and several THO subunits as well as accessory proteins (Dufu *et al.*, 2010; Moon *et al.*, 2011; Gewartowski *et al.*, 2012). A plant THO core complex, similar to the metazoan THO/TREX complex, has been identified in Arabidopsis. It consists of at least eight proteins: THO1/HPR1/EMU, THO2, THO3/TEX1, THO4, THO5, THO6, THO7 and UAP56 (Furumizu *et al.*, 2010; Jauvion *et al.*, 2010; Yelina *et al.*, 2010). Mutations in the Arabidopsis *TEX1*, *THO6* and *THO1* genes cause a reduction in the siRNA levels from *TAS* genes, inverted repeat (IR) genes and transgenes (Jauvion *et al.*, 2010). The *tho1* mutant alleles were also found to affect the alternative splicing patterns of transcripts encoding serine/arginine-rich proteins (Furumizu *et al.*, 2010).

To date, the functional specialization of other plant THO components in plants has not been fully dissected. Among them is the core component THO2, which we investigated here. The yeast gene encoding THO2 was first identified as a gene affecting transcription elongation of HYPERRECPMBINATION PROTEIN 1 (HPR1) (Piruat and Aguilera, 1998). In Arabidopsis, null mutations in *THO2* cause embryo lethality, whereas null mutations in *THO1* and *TEX1* (*hpr1* and *tex1*, respectively) cause developmental defects including dwarf stature, leaf serration, curly leaves and embryonic defects (Furumizu *et al.*, 2010; Jauvion *et al.*, 2010; Yelina *et al.*, 2010). The embryo lethality of *tho2* mutants suggests that THO2 has essential roles that go beyond those of other members of the complex. However, that lethality is a major problem with respect to the study of THO2 functions, and has hampered our understanding of the functional specialization of THO2.

Here we elucidated the function of Arabidopsis *THO2* by exploring a set of five mutant alleles ranging from null to hypomorphic. The identification of viable *tho2* mutant alleles allowed us to study the functions of THO2. We showed that plants containing mutations in the *THO2* gene present serious developmental defects, with failures in all the small RNA pathways that we examined, including miRNAs, tasiRNAs and siRNAs. As a consequence of the reduced production of miRNA, a feedback mechanism is triggered, increasing the amount of miRNA precursors and causing a concomitant over-accumulation of miRNA-targeted mRNAs. We found that THO2 does not appear to interact with any of the known miRNA biogenesis components, but rather with the splicing machinery, implying an indirect role of THO2 in small RNA biogenesis. Our studies showed that THO2 interacts with miRNA precursors, assisting their transport into the miRNA-processing complex. In *tho2* mutant plants, the miRNA precursors fail to associate

with the processing complex, specifically with HYL1, explaining the reduction in miRNA production observed in this mutant background. We also found that alternative splicing was compromised in *tho2* mutants, possibly reflecting a second conserved role for THO2. The severity and multiplicity of the molecular pathways affected in *tho2* mutants may explain why mutations in this gene cause more severe developmental problems than the lack of any other component of the THO/TREX complex.

RESULTS

Identification and characterization of several Arabidopsis *THO2* mutants

The study of the biological functions of THO2 was particularly challenging until now because no homozygous *tho2* alleles had yet been isolated. Previously studied T-DNA mutant lines for *THO2*, specifically the *tho2-1* (SALK_072011c) and *tho2-2* (SALK_130342) mutants, aborted at embryonic stages (Furumizu *et al.*, 2010; Jauvion *et al.*, 2010; Yelina *et al.*, 2010). These mutants feature T-DNA insertions in exons 16 and 18, respectively (Figure 1a). Consistent with these previous reports, we failed to identify mature plants homozygous for these alleles. However, we observed a population of tiny seedlings, which accounted for approximately 6% of the *tho2-1* and *tho2-2* segregation populations, after seeds were sown on MS plates. These seedlings never developed true leaves, had very short roots, failed to develop and died (Figure 1b,c). PCR analysis confirmed that all these tiny seedlings were homozygous for T-DNA insertions at the *THO2* locus (Figure 1d). These results showed that even though most *tho2-1* and *tho2-2* homozygous embryos abort, some reached very early developmental stages and may be used for further experimentation.

Recently a genetic screen using an artificial microRNA (amiRNA) targeting the luciferase reporter gene was performed to identify proteins acting in the miRNA pathway (Manavella *et al.*, 2012a). Whole-genome sequencing followed by SHORE mapping allowed mapping of the locus responsible for the miRNA dysfunction in one of the isolated mutant plants to chromosome 1, where a new polymorphism in the *THO2* (*At1g24706*) gene was identified. This mutant, *tho2-5*, contains a C→T mutation that results in a non-synonymous substitution of serine by phenylalanine (Figure 1a). The *tho2-5* plants showed a dwarf stature and narrow curly leaves, and produced few seeds (Figure 2a–c). Transformation of the mutants with the wild-type *THO2* cDNA, driven by its own promoter and fused to mCitrine, restored silencing of the luciferase reporter and reversed the *tho2-5* morphological defects, confirming that the mutation in *THO2* is the cause of the observed phenotype (Figure 2a–c). A second mutant, *tho2-6*, was isolated from an activation tagging screening performed in our laboratory. The position of the T-DNA insertion was estab-

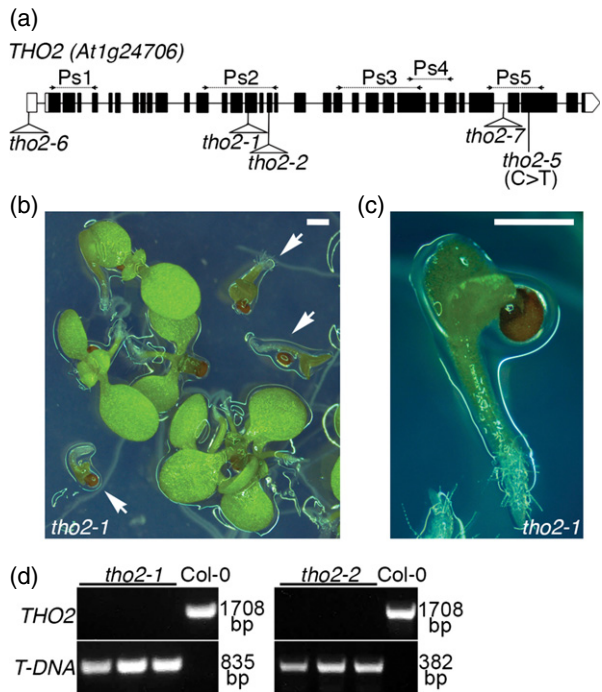


Figure 1. Identification of *thox2-1a* and *thox2-2* homozygous plants. (a) Gene structure of *THO2* (At1g24706) showing single nucleotide substitution and T-DNA insertion sites in *thox2-1*, *thox2-2*, *thox2-5*, *thox2-6* and *thox2-7*. Black boxes and lines represent exons and introns, respectively; white boxes represent 5' and 3' UTRs. Arrows indicate the position of primer sets used for RT-PCR analysis in Figure 5(a). (b) Fourteen-day-old seedlings of *thox2-1* grown on an MS plate, showing arrested growth. Arrows indicate *thox2* homozygous seedlings. Scale bar = 1 mm. (c) Magnified view of homozygous seedling shown in (b). Scale bar = 1 mm. (d) PCR genotyping of homozygous *thox2-1* and *thox2-2* seedlings.

lished by TAIL-PCR, and mapped to the 5' UTR of *THO2* (Figure 1a). Segregation analysis and PCR-assisted genotyping allowed us to isolate homozygous *thox2-6* plants that contain a single copy of the T-DNA insertion. These mutant plants developed curly leaves and had a bushy reduced stature (Figure 3a–c). The plants present an abnormal distribution of petals (Figure 3d), atrophic anthers that fail to produce mature pollen grains leading to complete sterility (Figure 3e), fusion of the carpels that form twisted pistils

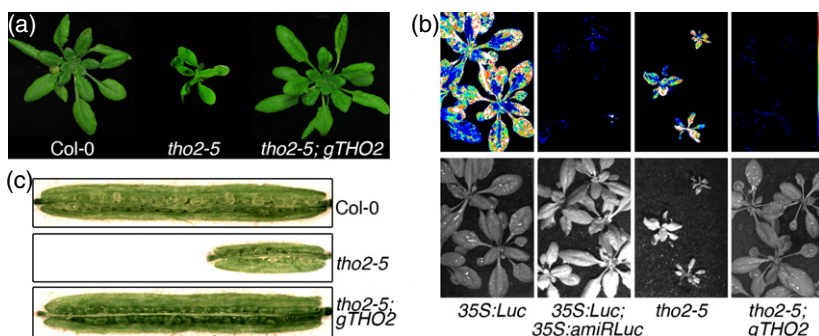


Figure 2. Isolation and characterization of *thox2-5*. (a) Phenotype of 20-day-old Col-0, *thox2-5* mutant and complemented plants. (b) Bioluminescence phenotype of *thox2-5* mutants, complemented mutants, reporter lines (35S:Luc;35S:amiRLuc) and Pro35S:LUC controls. The upper panels show bioluminescence activity; the colored scale indicates low luminescence (blue) to high luminescence (white). The lower panels show bright-field images of the same plants. (c) Dissected siliques of Col-0, *thox2-5* and the complemented mutant.

exposing the ovules (Figure 3f), and a large number of trichomes in the floral buds (Figure 3g). Inspection of dissected siliques from heterozygous plants revealed that 15% of the ovules ($n = 553$), which are probably homozygous for the T-DNA insertion, aborted (Figure 3h,i).

Additionally, we analyzed an uncharacterized *thox2* allele (SALK_144229) that contains a T-DNA insertion in intron 30 towards the end of the gene (Figure 1a). Plants homozygous for this allele, named *thox2-7*, were able to reach maturity, showing small stature, serrated leaves, an increased number of trichomes on their sepals, and short anther filaments and pistils (Figure 4a–f). Approximately 5% of the flowers of mutant plants had five petals (Figure 4d). Their fertility was reduced to less than 20% compared to heterozygous plants due to embryonic abortion (Figure 4h,i).

Expression of *THO2* in wild-type and mutant Arabidopsis plants

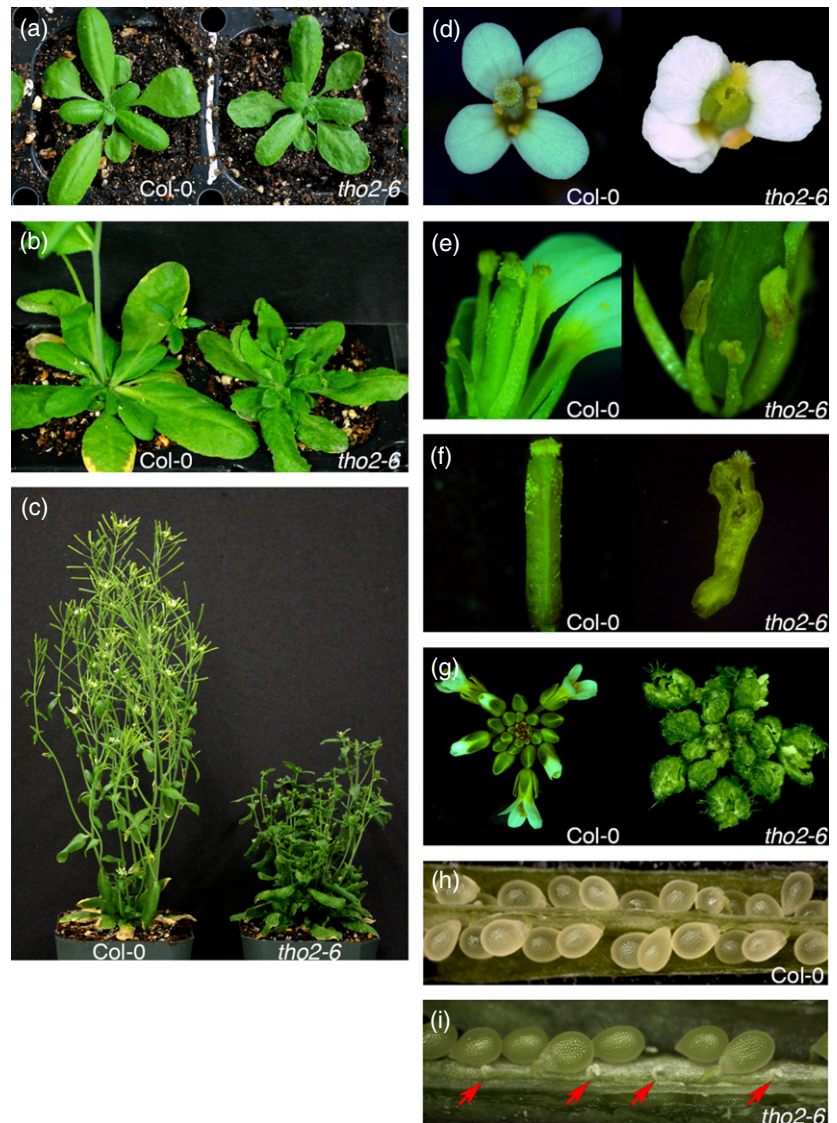
RT-PCR expression analysis of *THO2*, using primers sets designed to flank the mutation sites (Figure 1a), revealed that *thox2-1*, *thox2-2* and *thox2-7* produced truncated versions of the *THO2* mRNA (Figure 5a). *thox2-6* showed intact but strongly reduced levels of *THO2* mRNA, while *thox2-5*, as expected from plants with a non-synonymous point mutation, showed no change in the abundance or size of the mRNA (Figure 5a). Considering the mutant phenotypes, it is conceivable that *thox2-1* and *thox2-2* are null alleles, *thox2-6* is a knockdown allele, and *thox2-5* and *thox2-7* may become very useful tools to study the biological function of *THO2*, the core protein of the THO/TREX complex. RT-PCR experiments showed that, in wild-type plants, *THO2* is expressed at very similar levels in the flower buds, mature flowers, stems, leaves, roots and whole seedlings, as well as in pollen at all developmental stages, including isolated spores, unicellular, bicellular and tricellular phases, and mature pollen (Figure 5b).

THO2 is required for accumulation of miRNAs, tasiRNAs and siRNAs

Components of the Arabidopsis THO/TREX complex, such as *TEX1* and *THO1*, have been described as important part-

Figure 3. Phenotypic characterization of *tho2-6* mutant plants.

(a) *tho2-6* and Col-0 plants at the early rosette-leaf stage.
 (b) Leaf proliferation and delayed bolting in *tho2-6* plants.
 (c) *tho2-6* and wild-type plants at 42 days old.
 (d–g) Flowers, anthers, pistils and inflorescences of wild-type and *tho2-6* plants.
 (h, i) Dissected siliques of wild-type and *tho2-6* plants. Red arrows indicate aborted ovules.



ners in several small RNA pathways (Furumizu *et al.*, 2010; Jauvion *et al.*, 2010; Yelina *et al.*, 2010). To test whether *THO2* is involved in siRNA biosynthesis, we crossed *tho2* mutants (*tho2-6* and *tho2-7*) with *JAP3* transgenic lines. These transgenic plants express an inverted repeat version of the PHYTOENE DESATURASE (*PDS*) gene under the control of the phloem-specific *SUC2* promoter (*SUC2p*:*PDS*-IR; Smith *et al.*, 2007). *JAP3* plants exhibit a unique phenotype of photo-bleaching around the leaf veins, consequence of the silencing of the *PDS* gene by the *SUC2p*:*PDS*-IR construct. Segregation analysis and PCR-assisted genotyping revealed that wild-type plants or plants heterozygous for the *tho2-6* and *tho2-7* alleles retain the typical *JAP3* photobleaching phenotype (Figure 6a). In contrast, all plants homozygous for the mutations completely lost the photobleaching phenotype and showed the typical *tho2-6* or *tho2-7* leaf shape (Figure 6a). Quantitative RT-

PCR analyses demonstrated that the level of *PDS* transcripts was higher in the *JAP3/tho2-6* and *JAP3/tho2-7* plants than in the original *JAP3* line (Figure 6b). This over-accumulation of the *PDS* transcript correlated with a reduction in *PDS*-derived siRNAs observed in both the *tho2-6* and *tho2-7* mutant backgrounds (Figure 6c).

As the *tho2-5* allele was isolated from a miRNA-activity based screening, we wished to determine whether *THO2* also has a role in the miRNA pathway. To determine whether *THO2* is required for miRNA biogenesis or action, we evaluated the steady-state levels of mature miRNAs and miRNA-targeted mRNAs in *tho2* mutants by Northern blotting and quantitative RT-PCR, respectively. We found that miRNA levels were strongly reduced in all tested *tho2* mutants, with the exception of *tho2-7*, which showed normal miRNA levels (Figure 6d). Interestingly, no changes were detected for miR171, which suggests that *THO2* is not

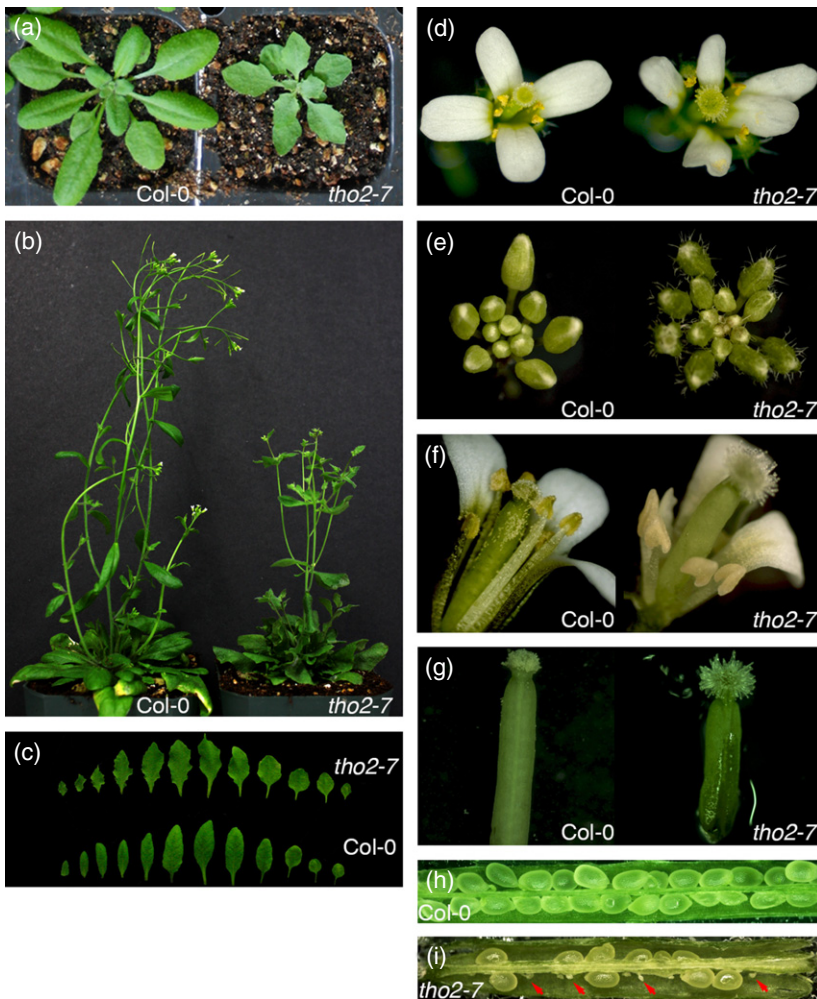


Figure 4. Phenotypic characterization of *tho2-7* mutant plants.

(a) *tho2-7* and Col-0 plants at the early rosette-leaf stage.

(b) *tho2-7* and Col-0 wild-type plants at 42 days old.

(c) Leaf series of *tho2-7* showing serration of leaf edges compared with wild-type leaves.

(d–g) Flowers, inflorescences, anthers and pistils of wild-type and *tho2-7* plants.

(h, i) Dissected siliques of wild-type and *tho2-7* plants. Red arrows indicate aborted ovules.

involved in generation of this miRNA. The reduction in miRNA levels was paralleled by higher accumulation of several miRNA-target mRNAs (TCP3 targeted by miR319; MYB33 targeted by miR159; ARF8 targeted by miR167; AP2 and TOE2 targeted by miR172) (Figure 6e). All tested *tho2* mutant alleles showed higher levels of miRNA precursors than wild-type plants (Figure 6f). Such accumulation of miRNA precursors is a common transcriptional feedback response to low mature miRNA levels, as observed in plants mutated in other miRNA biogenesis factors (Song *et al.*, 2007; Laubinger *et al.*, 2008; Ben Chaabane *et al.*, 2013; Wu *et al.*, 2013). The primers used to detect miRNA precursors in this work cannot distinguish between pri-miRNA and pre-miRNA sequences. We have used the term miRNA precursors as a general term to refer to both RNA intermediate molecules. As shown for mutants of other THO/TREX complex components (Jauvion *et al.*, 2010; Yelina *et al.*, 2010), all tested *tho2* mutants showed a marked reduction in secondary siRNA derived from *TAS1* and endogenous siRNA (Figure 6d). We observed that inclusion of a *THO2* genomic fragment in the *tho2-5* mutant back-

ground reverses the reduction in small RNAs, thus confirming that THO2 is responsible for this phenotype (Figure S1a). For both the RNA blots (Figure 6d) and the quantitative RT-PCR experiments (Figure 6e,f) we used *hyl1-2* mutants as control plants. Mutants in *hyl1* show reduced production of miRNAs, over-accumulation of miRNA precursors, and a concomitant increase in miRNA-targeted transcripts (Han *et al.*, 2004; Song *et al.*, 2007).

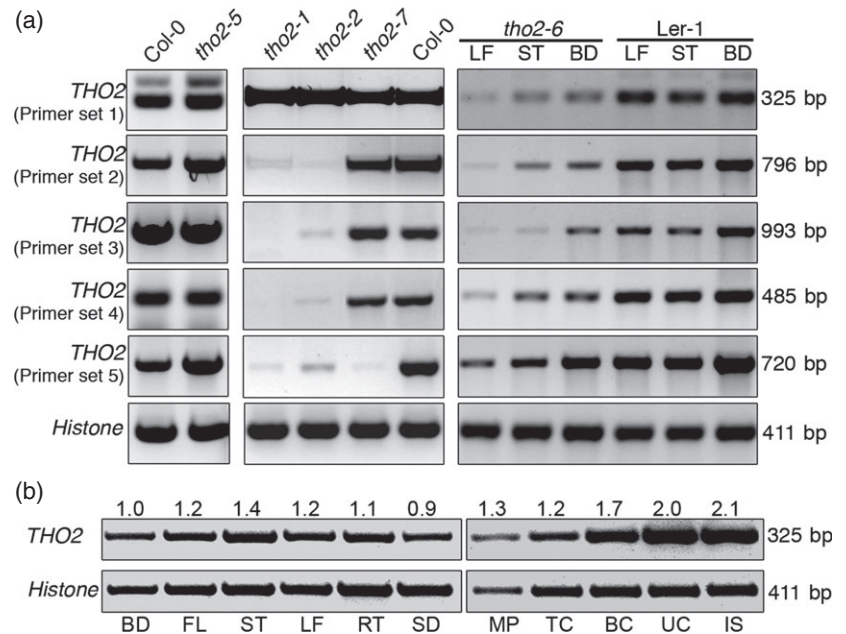
THO2 is associated with miRNA precursors and is required for their recruitment into the miRNA-processing complex

With the aim of understanding how THO2 acts in the miRNA pathway, we co-transformed plants with THO2:eGFP and HYL1:mCherry constructs, and observed the localization of the proteins using a confocal microscope. Our observations revealed that THO2 accumulated in the nucleus, specifically in nuclear speckles different to those in which the miRNA biogenesis machinery is located (Figure 7a). The same nuclear expression pattern was observed for *tho2-5* mutants rescued using the gTHO2:mCitrine construct (Figure S1b). In accordance with this

Figure 5. Expression of *THO2*.

(a) Expression of *THO2* measured by RT-PCR in *tho2-1*, *tho2-2*, *tho2-5*, *tho2-6* and *tho2-7* plants. For *tho2-6*, tissues from leaf (LF), stem (ST) and floral buds (BD) were analyzed. Histone was used as a loading control. The positions of primer sets used for the analysis are shown in Figure 1(a).

(b) RT-PCR analysis of *THO2* expression in Col-0 floral bud (BD), open flower (FL), stem (ST), leaf (LF), root (RT), and whole seedling (SD), and at different developmental stages of Col-0 pollen: mature pollen (MP), pollen in tricellular (TC), bicellular (BC), unicellular (UC) phases and isolated spores (IS). Histone was used as control.



observation, we were not able to detect any interaction in a yeast two-hybrid interaction screen using *THO2* fused to GAL4-BD and a collection of 18 known small RNA-related proteins fused to GAL4-AD (Figure S2).

The facts that *THO2* does not interact with any miRNA biogenesis factor and that it is also involved in other small RNA pathways suggests that it may act in early steps that are common to all these pathways, such as transport or stabilization of the primary double-stranded RNA precursors. In order to test whether *THO2* associates with miRNA precursors, we used *THO2:eGFP* transgenic plants to immunoprecipitate the fusion protein and search for associated RNA molecules. After selecting plants by fluorescent microscopy, we pulled down the *THO2:eGFP* fusion using an anti-GFP antibody. Total or *THO2*-associated RNA was extracted from the input and immunoprecipitate fractions, and used to synthesize cDNA. RT-PCR experiments revealed that all tested miRNA precursors associate with *THO2* (Figure 7b). We then evaluated whether the observed association is important for recruitment of miRNA precursors into the processing complex. In order to test this scenario, we evaluated the HYL1-associated miRNA precursors by using an anti-HYL1 antibody to co-immunoprecipitate the protein in the *tho2-5* mutant background. Interestingly, we found a reduction in the HYL1-associated miRNA precursors in *tho2-5* plants (Figure 7c,d) despite these mutants containing more pri/pre-miRNAs than wild-type plants (Figure 6f). The association of *THO2* with miRNA precursors and the reduced association with HYL1 observed in the *tho2-5* background suggest a role for *THO2* in transport of these RNA molecules to the processing complex or in their stabilization. Interestingly,

the precursors of miR171a, which were not drastically reduced in *tho2* mutant plants (Figure 6d), appeared to be poorly associated with *THO2* (Figure 7b). In *tho2-5* mutants, the level of HYL1-associated miR171a precursors appeared unchanged compared to wild-type plants (Figure 7c,d), suggesting an alternative pathway for this miRNA.

THO2 is required for splicing in Arabidopsis plants

In humans, the *THO/TREX* complex is involved in splicing through interaction with the spliceosomes (Rappsilber *et al.*, 2002). In Arabidopsis, it has been shown that mutations in the *emu/tho1* locus affect the alternative splicing of genes encoding serine/arginine-rich (SR) proteins (Furumizu *et al.*, 2010). Supporting this reported role of the *THO/TREX* complex during mRNA splicing, we detected a partial overlap between the nuclear localization of *THO2* and SRp34, a canonical spliceosome component (Figure 7e). Despite sharing localization in the same nuclear speckles, *THO2* also localized in the cell nucleolus, a feature that is not shared with SRp34, suggesting additional roles of *THO2*. We also performed RT-PCR using mRNAs extracted from *tho2* seedlings to determine the splicing patterns of several SR genes encoding proteins involved in RNA splicing. Our analysis indicated that, of all tested SR genes, only *SR34b* showed a differential splicing pattern in all *tho2* alleles compared to wild-type plants (Figures 7f and S3a). To further examine the alternative splicing patterns of *SR34b*, we used capillary electrophoresis to analyze the splicing isoforms in samples from the *tho2-6* mutant. Double-stranded DNA derived from the splicing fragments was generated by RT-PCR and separated in a

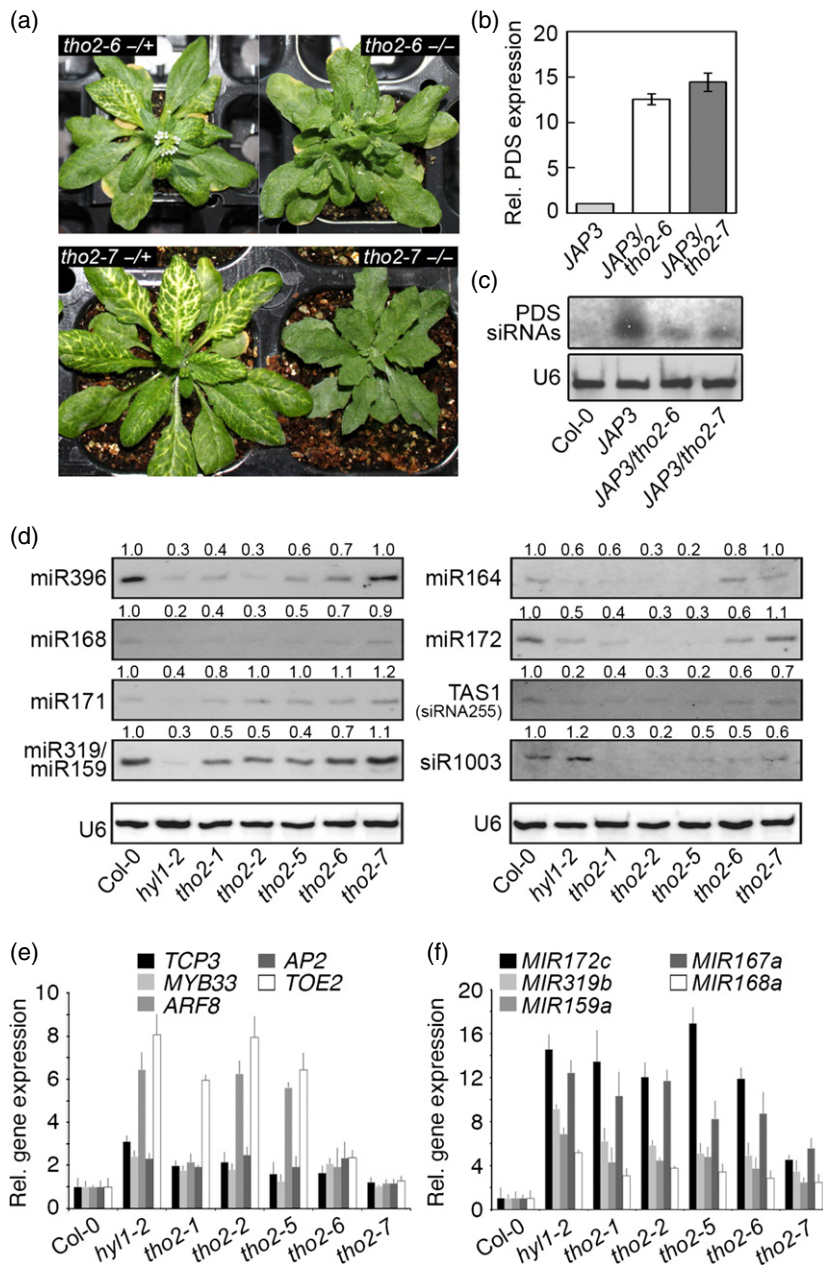


Figure 6. Effects of mutation in *THO2* on accumulation of small RNAs.

(a) Phenotypes of the *JAP3/tho2-6* and *JAP3/tho2-7* mutants.

(b) Quantitative RT-PCR analyses of *PDS* expression in *JAP3*, *JAP3/tho2-6* and *JAP3/tho2-7* plants. Error bars indicate 2 × standard error of the mean (SEM).

(c) RNA blots for *PDS*-derived siRNAs. The U6 small nuclear RNA (U6) was used as a loading control.

(d) RNA blots for detecting miRNAs, TAS1-derived tasiRNAs (siRNA 255) and siR1003. U6 was used as a loading control. The relative abundance of small RNAs was calculated by measuring the band intensity using ImageJ (<http://imagej.nih.gov/ij/>), and is indicated above each band.

(e, f) Quantitative RT-PCR analysis of miRNA targets and miRNA precursors. Error bars indicate 2 × standard error of the mean (SEM).

capillary electrophoresis device. The resulting pattern for each sample reflects the sizes of the observed splicing forms. The analysis confirmed the differential splicing pattern of *SR34b* in *tho2-6* mutants, clearly showing a shift to smaller transcript fragments in the mutant (Figure 7g). We did not find any difference in the splicing pattern of intron-containing or intron-contained miRNA genes between mutant and wild-type plants (Figure S3b). Given these findings, it is possible that aberrant splicing or mRNA destabilization of general small RNA factors may generate a reduction in miRNA biogenesis, contributing to the observed miRNA reduction. Alternatively, given the *THO*/

TREX function in mRNA transport, it may be possible that the mRNAs of miRNA-related factors fail to reach the ribosomes, and thus are not translated. Quantitative RT-PCR analysis showed no significant difference in the mRNA accumulation of several miRNA factors (Figure S4a). We only detected a slight increase in *AGO1* mRNA in the mutant plants, probably a consequence of the reduction in miR168, thus discounting a mRNA destabilization scenario. RT-PCR analysis of the mRNAs of miRNA-related factors showed no differential splicing patterns between wild-type and mutant plants, at least for tested regions of the transcripts (Figure S4b). Such observations discount the possi-

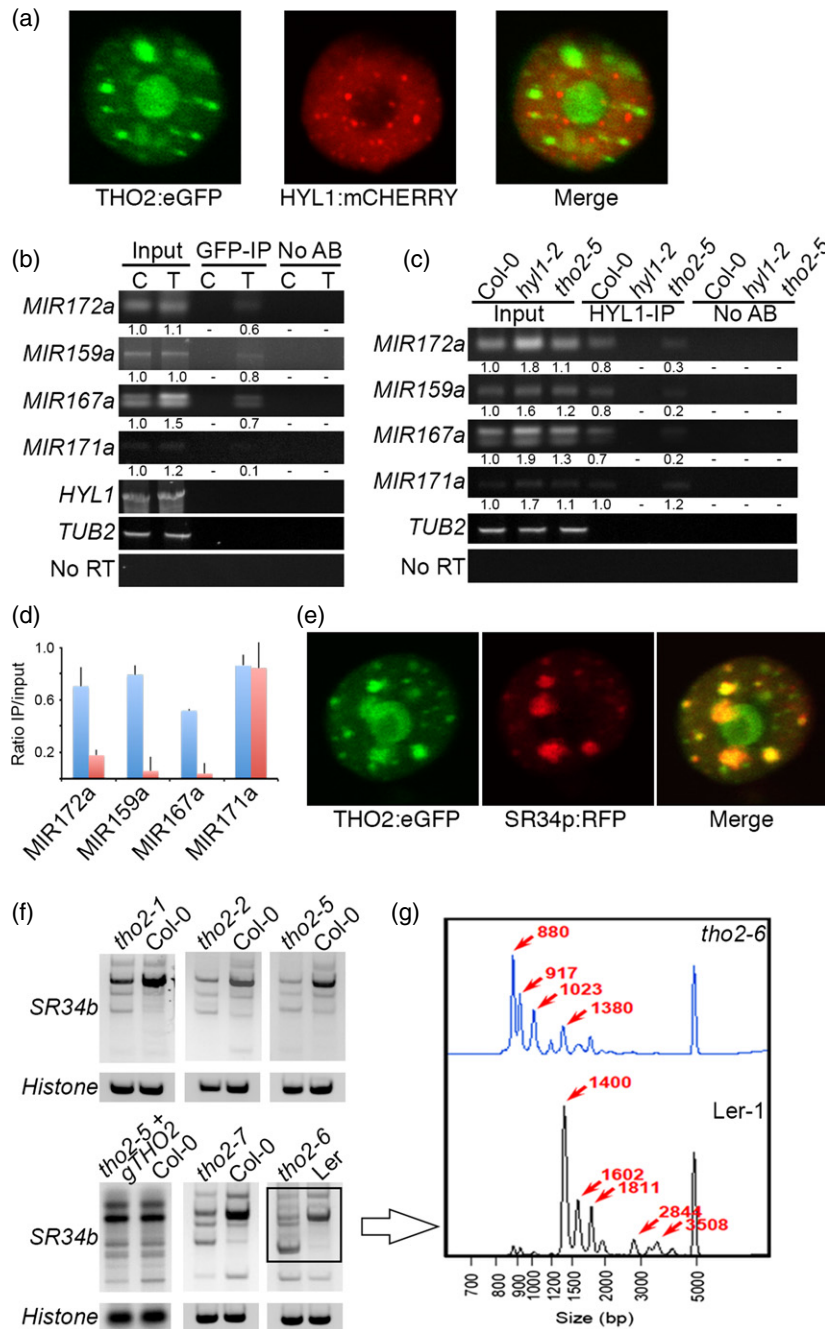


Figure 7. THO2 binds miRNA precursors, delivers them to the processing complex, and regulates mRNA splicing in Arabidopsis.

(a) Confocal microscopy images showing the nuclear localization of THO2:eGFP and HYL1:mCherry.

(b) RT-PCR to detect THO2-associated miRNA precursors in RNA immunoprecipitation samples. C, 3xGFP:NLS transgenic plants were used as a negative control for un-specific binding. T, THO2:eGFP transgenic plants. Lanes 5 and 6 ('No AB') show RT-PCR performed on samples to which no antibody was added during the RNA immunoprecipitation protocol. RT-PCR measurement of HYL1 mRNA was performed to exclude un-specific binding of THO2. β -TUBULIN2 mRNA was used as a control mRNA. The 'No RT' control was performed using a mixture of primers amplifying the miR159a, 167a, 171a and 172a precursors. Band intensity was quantified using ImageJ, and is indicated below each band.

(c) RNA immunoprecipitation assay performed using an anti-HYL1 antibody.

(d) Quantitative RT-PCR analysis of the RNA immunoprecipitation miRNA precursors. Data are expressed as a ratio between the immunoprecipitate and input fractions for Col-0 plants (blue bars) and *tho2-5* mutants (red bars). Expression levels were normalized against the levels of β -TUBULIN2 (At5g62690) in the input fraction. Error bars indicate $2 \times$ standard error of the mean (SEM).

(e) Confocal microscopy images showing partial co-localization of THO2:eGFP and SR34p:RFP.

(f) RT-PCR analysis of splicing patterns of SR34b in wild-type, *tho2* mutants and *tho2-5* complemented mutants (*tho2-5*+ gTHO2). Histone was used as a loading control.

(g) Splicing isoforms of SR34b generated in *tho2-6* and Col-0 were analyzed via capillary electrophoresis. Various sizes of isoforms (in bp) are indicated.

bility that aberrant splicing of miRNA biogenesis factors contributes to the reduction in their production. Finally, Western blotting using antibodies against HYL1, AGO1 and DCL1 revealed no significant change in the accumulation of these proteins in the mutant plants (Figure S4c). These results indicate that, at least for these miRNA-related genes, mRNA translation is not affected in the mutants. The observed over-accumulation of AGO1 in the *tho2-5* mutant may potentially reflect loss of the miR168-AGO1 regulation node.

ABA HYPERSENSITIVE 1 (ABH1), CAP-BINDING PROTEIN 20 (CBP20) and DAWDLE (DDL) are miRNA biogenesis co-factors involved in mRNA splicing and miRNA precursor stabilization (Kim *et al.*, 2008; Laubinger *et al.*, 2008; Yu *et al.*, 2008). The overlap between these proteins and THO2 functions led us to speculate whether THO2 interacts with them. However, our yeast two-hybrid results indicated that THO2 does not interact, at least directly, with ABH1, CBP20 or DDL (Figure S5). In any case, these results do not exclude the possibility that the THO/TREX complex, once fully assembled, interacts with these proteins to fulfill its miRNA-related functions.

DISCUSSION

The THO/TREX complex is highly conserved in multiple organisms, acting in various contexts. In humans, it is a key component of the mRNA export machinery, and appears to be primarily associated with spliced mRNA (Masuda *et al.*, 2005; Chi *et al.*, 2013). THO2 is the largest protein of the complex, and is considered to be its core (Pena *et al.*, 2012). Based on the fact that *THO2* null mutants in *Arabidopsis* die at the embryonic stage, it has been proposed that the protein is essential for assembly of the complex and its function, and therefore for the survival of the plant (Furumizu *et al.*, 2010; Jauvion *et al.*, 2010; Yelina *et al.*, 2010). The isolation of viable *tho2* alleles, described in the present work, is a major breakthrough for study of the THO/TREX complex. Despite developmental defects, ranging from abnormal floral organs and leaf serrations to partial embryo lethality, observed in the newly characterized *tho2-5*, *tho2-6* and *tho2-7*, these mutants represent a unique genetic tool for studying THO2, the core protein of the THO/TREX complex (Pena *et al.*, 2012).

As observed in mutant plants for other components of the THO/TREX complex, *tho2* mutants show reduced siRNA-mediated silencing, with a concomitant reduction in the steady-state levels of siRNAs and tasiRNAs. We also observed reduced levels of mature miRNAs and over-accumulation of miRNA-targeted mRNAs in the *tho2* mutant plants (Figure 6). Previous reports have shown that other components of the complex, such as THO1, regulate miRNA accumulation (Furumizu *et al.*, 2010). However, TEX1, which is required for siRNA and tasiRNA production, does not appear to be involved in the miRNA pathway (Yelina

et al., 2010). Our data show that the *tho2* mutants present morphological and molecular phenotypes more severe than those observed in mutants for other THO/TREX components (Furumizu *et al.*, 2010; Jauvion *et al.*, 2010; Yelina *et al.*, 2010). This observation suggests that THO2 is central for the functionality of the complex, while each accessory protein may have a more specific function. This is supported by the extreme phenotype of the *tho2* mutants and the embryonic lethality of the *THO2* null alleles. It is probable that, in the absence of THO2, but not of the other components, the whole complex fails to assemble. However, more experimentation is required to confirm this. Interestingly, the *tho2-7* mutation, which generates a truncated messenger lacking the very last portion of the gene, does not lead to any alteration in miRNA accumulation, but still induces reduction of tasiRNAs, siRNA silencing and alternative splicing similar to what is observed for the other alleles (Figures 6 and 7). This may indicate that the missing portion of THO2 is, either by itself or through an interacting partner, dispensable for the miRNA regulation but essential for the other small RNA molecules. A potential candidate in this last scenario is TEX1, as it has been described as not being required for miRNA accumulation, but its mutation drastically affects both the accumulation of tasiRNAs and SUC2p:PDS transgene siRNAs (Smith *et al.*, 2007; Yelina *et al.*, 2010). However, it has been reported in yeast that the C-terminal region of the THO2 protein, a poorly conserved region of the protein, interacts with nucleic acids but has little effect on the integrity of the complex (Pena *et al.*, 2012).

Despite many studies examining the function of the plant THO/TREX complex, it remains unclear how the complex acts in small RNA pathways. Using a yeast two-hybrid approach, we observed that THO2 did not interact with any of the tested miRNA processing components (Figures S1 and S5). This observation, together with the fact that THO2 is found in a different subcellular localization to the miRNA processing factors, suggests that the effect on this pathway is not at the miRNA processing level. This idea is in agreement with the possibility that THO2 acts in multiple small RNA pathways. It has been proposed that the THO/TREX complex is required for transporting siRNA/tasiRNA precursors to an unknown subcellular location for their processing (Yelina *et al.*, 2010). This is consistent with the known function of the complex in mRNA trafficking in fungi and metazoans (Reed and Cheng, 2005). In the present work, we show experimental evidence supporting such a scenario. We show that THO2 is able to interact with miRNA precursors, an interaction that appears to be important for recruitment of these molecules to the processing complex. The fact that *tho2* mutants fail to accumulate several classes of small RNAs may suggest that the complex has a broad affinity for a common component of all these pathways. Thus it is possible that the THO/TREX complex

recognizes and transports double-stranded RNA, which, despite the difference in their origin and nature, is a common feature of all small RNA precursors. Results obtained in previous reports (Furumizu *et al.*, 2010; Jauvion *et al.*, 2010; Yelina *et al.*, 2010) suggest that each individual component of the THO/TREX complex in plants, other than THO2, specifically affects a small RNA pathway, probably by differential preference for precursors.

In recent years, it has become evident that the miRNA pathway is linked or at least affected by the splicing machinery. Proteins such as SE, the cap-binding complex and TOUGH have been found to play roles in miRNA biogenesis and alternative splicing in Arabidopsis (Kim *et al.*, 2008; Laubinger *et al.*, 2008; Ren *et al.*, 2012). Our results revealed similar dual roles for THO2. Not surprisingly, the weak loss-of-function alleles of *tho2* display morphological defects similar to *se*, *cbp80*, and *cbp20* mutants, while both *se* and *tho2* null mutants die at embryonic stages (Hugouvieux *et al.*, 2001; Bezerra *et al.*, 2004; Papp *et al.*, 2004). We found that THO2 shared nuclear localization with the canonical splicing factor SR34p, and identified a case of abnormal alternative splicing in the *tho2* mutants. A genome-wide analysis of alternative splicing in plants mutated in each of the genes encoding components of the complex is required in order to understand how this process is affected by dysfunction of the complex.

EXPERIMENTAL PROCEDURES

Plant materials and growth conditions

The *tho2-5* mutant was isolated in a previously described forward-genetics screen (Manavella *et al.*, 2012a). *tho2-1* (SALK_072011), *tho2-2* (SALK_130342) and *tho2-7* (SALK_144229) were obtained from the Arabidopsis Biological Research Center (<https://abrc.osu.edu/>). The *tho2-6* mutant was isolated from an Arabidopsis thaliana Landsberg erecta (*Ler*) activation tagging screen performed using the pSKI015 vector as previously described (Weigel *et al.*, 2000). All seeds were sown on soil or MS plates, and were cold-treated in the dark for 3 days before transfer to growth chambers under long-day conditions (16 h light/8 h of dark) at 22°C/20°C (day/night). PCR primers used to genotype *tho2* alleles are listed in Table S1.

Transgenes

The miRNA-reporter transgenic lines (35S:Luc;35S:amiRLuc) and control lines (35S:Luc) have been described previously (Manavella *et al.*, 2012b). A triple GFP construct with nuclear localization signal (3xGFP:NLS) has been described previously (Mathieu *et al.*, 2007). THO2:eGFP and HYL1:mCHERRY constructs were obtained by RT-PCR-mediated cDNA amplification, cloning into pCR8GW-TOPO (Life Technologies, www.lifetechnologies.com), and recombined into modified pGREEN vectors under the control of the CaMV 35S promoter to generate C-terminal fusions with the fluorescent proteins. The SRp34:RFP construct has been described previously (Lorkovic *et al.*, 2004). The THO2 genomic construct (gTHO2), used to rescue *tho2-5* mutants, was generated by fusing the PCR-amplified THO2 cDNA and a 2000 bp fragment upstream

of the THO2 transcription start site. The obtained product was cloned into pCR8GW-TOPO, and recombined into a modified pGREEN vector to generate a mCitrine C-terminal fusion. Yeast two-hybrid constructs were obtained by cloning the specific cDNAs into pCR8GW-TOPO, followed by recombination into the pDEST32 or pDEST22 vectors (Life Technologies). Arabidopsis thaliana JAP3 and *tho2-5* mutant plants were transformed using the flower-dip method (Clough and Bent, 1998). Transgenic seedlings were selected using 50 mg ml⁻¹ kanamycin on plates or 0.1% ammonium glufosinate on soil. At least 15 T₁ seedlings were analyzed for each construct. Transient infiltration of *Nicotiana benthamiana* leaves was performed as described previously (de Felippes and Weigel, 2010).

TAIL-PCR analysis

Genomic DNA samples were prepared from young leaves using a modified cetyl trimethyl ammonium bromide method (Murray and Thompson, 1980). To determine the sequences flanking the T-DNA insertion, we used nested pSKI015-specific primers (TR1, TR2, and TR3) and an arbitrary degenerate primer (P7) as described by Liu *et al.* (1995). The resulting PCR products were sequenced. The right border region was located using RB1, RB2 and RB3 primers. All primer sequences used are listed in Table S1.

Expression analysis

Total RNA was extracted using an RNeasy plant mini kit (Qiagen, www.qiagen.com) according to the manufacturer's instructions. Primers for RT-PCR and quantitative RT-PCR were designed in the intron flanking regions. cDNA synthesis from 1 µg total RNA was performed using an ImpromII reverse transcription system kit (Promega, www.promega.com/), with an oligo(dT) primer, according to the manufacturer's instructions. Quantitative RT-PCR, small RNA gel blots, confocal microscopy and luciferase measurements were performed as previously described (Manavella *et al.*, 2012b). RNA blots to detect PDS-derived siRNAs were performed using a radioactively labeled PCR-amplified fragment of the PDS gene as probe. Primers used for quantitative PCR and as RNA probes are listed in Table S1. Western blot analysis was performed using anti-HYL1, anti-DCL1 and anti-AGO antibodies (Agrisera, www.agrisera.com/) as previously described (Manavella *et al.*, 2013).

Yeast two-hybrid assays and confocal microscopy

Yeast two-hybrid assays were performed using the ProQuest™ two-hybrid system (Life Technologies), according to the manufacturer's instructions. To reduce auto-activation of THO2, we added 40–120 mM 3-amino-1,2,4-triazole to the selection medium. For the microscopy experiments, *N. benthamiana* leaves were transiently co-transformed with a THO2:eGFP fusion and a HYL1:mCherry or SR34p:RFP fusion (de Felippes and Weigel, 2010), and imaged using a TCS SP2 confocal microscope (Leica, <http://www.leicamicrosystems.com/>) on day 3 after infiltration.

RNA immunoprecipitation assay

RNA immunoprecipitation experiments were performed as previously described (Terzi and Simpson, 2009). Fifteen-day-old THO2:eGFP, 3xGFP:NLS, Col-0, *hyl1-2* and *tho2-5* plants were grown on MS agar plates. An anti-GFP antibody (Abcam, www.abcam.com), an anti-HYL1 antibody (Agrisera) and Protein G-agarose beads (Life Technologies) were used to immunoprecipitate protein-RNA complexes. After elution of protein-RNA complexes, RNA and proteins were extracted using TriPure reagent (Roche, <http://www.roche.com>).

www.roche.com). First-strand cDNA and RT-PCR of the associated RNAs were performed as described above.

Splicing fragment analysis

RT-PCR fragments were analyzed using a Fragment Analyzer™ automated CE system (Advanced Analytical Technologies, <http://www.aati-us.com/>). Diluted samples (1/10) were prepared using a DNF-910/15L80M dsDNA reagent kit (Advanced Analytical Technologies), according to the manufacturer's instructions. Separation results were analyzed using PROSize® 2.0 software (Advanced Analytical Technologies).

ACKNOWLEDGMENTS

We thank Detlef Weigel, Moon-Soo Soh and Jong Tae Song for comments and discussion of the manuscript. This research was supported by grants from the Next-Generation BioGreen21 Program, Rural Development Administration, Republic of Korea (Plant Molecular Breeding Center number PJ008137/National Center for GM Crops number PJ01128401) (to S.K.P.), the Human Frontier Science Program (to P.A.M.), the Max Planck Society (to P.A.M. and P.L.) and the International Centre for Genetic Engineering and Biotechnology (to P.A.M.). P.A.M. is a member of the Consejo Nacional de Investigaciones Científicas y Técnicas (Argentina). We also thank David Baulcombe, University of Cambridge, Department of Plant Sciences, for the *JAP3* transgenic lines, Andrea Barta, Max F. Perutz Laboratories, Department of Medical Biochemistry, for the SRp34: RFP construct, and Xuemei Chen and Bin Yu, University of California Riverside, Department of Botany and Plant Sciences, for the pGAD10-DDL construct.

SUPPORTING INFORMATION

Additional Supporting Information may be found in the online version of this article.

Figure S1. miRNA accumulation in *tho2-5* complemented plants.

Figure S2. Yeast two-hybrid assay for testing the interaction of THO2 with a collection of miRNA-related factors.

Figure S3. Splicing patterns in *tho2* mutants.

Figure S4. Splicing patterns, mRNA and protein accumulation of miRNA biogenesis factors in *tho2* mutants.

Figure S5. Yeast two-hybrid assays for the interaction between THO2 and DDL, ABH1 or CBP20.

Table S1. Oligonucleotide sequences used in this study.

REFERENCES

- Baulcombe, D. (2004) RNA silencing in plants. *Nature*, **431**, 356–363.
- Ben Chaabane, S., Liu, R., Chinnusamy, V., Kwon, Y., Park, J.H., Kim, S.Y., Zhu, J.K., Yang, S.W. and Lee, B.H. (2013) STA1, an Arabidopsis pre-mRNA processing factor 6 homolog, is a new player involved in miRNA biogenesis. *Nucleic Acids Res.* **41**, 1984–1997.
- Bezerra, I.C., Michaels, S.D., Schomburg, F.M. and Amasino, R.M. (2004) Lesions in the mRNA cap-binding gene *ABA HYPERSENSITIVE 1* suppress *FRIGIDA*-mediated delayed flowering in *Arabidopsis*. *Plant J.* **40**, 112–119.
- Chapman, E.J. and Carrington, J.C. (2007) Specialization and evolution of endogenous small RNA pathways. *Nat. Rev. Genet.* **8**, 884–896.
- Chi, B., Wang, Q., Wu, G., Tan, M., Wang, L., Shi, M., Chang, X. and Cheng, H. (2013) Aly and THO are required for assembly of the human TREX complex and association of TREX components with the spliced mRNA. *Nucleic Acids Res.* **41**, 1294–1306.
- Clough, S.J. and Bent, A.F. (1998) Floral dip: a simplified method for *Agrobacterium*-mediated transformation of *Arabidopsis thaliana*. *Plant J.* **16**, 735–743.
- Dufu, K., Livingstone, M.J., Seebacher, J., Gygi, S.P., Wilson, S.A. and Reed, R. (2010) ATP is required for interactions between UAP56 and two conserved mRNA export proteins, Aly and CIP29, to assemble the TREX complex. *Genes Dev.* **24**, 2043–2053.
- Fang, Y. and Spector, D.L. (2007) Identification of nuclear dicing bodies containing proteins for microRNA biogenesis in living *Arabidopsis* plants. *Curr. Biol.* **17**, 818–823.
- de Felippes, F.F. and Weigel, D. (2010) Transient assays for the analysis of miRNA processing and function. *Methods Mol. Biol.* **592**, 255–264.
- Fujioka, Y., Utsumi, M., Ohba, Y. and Watanabe, Y. (2007) Location of a possible miRNA processing site in Smd3/Smb nuclear bodies in *Arabidopsis*. *Plant Cell Physiol.* **48**, 1243–1253.
- Furumizu, C., Tsukaya, H. and Komeda, Y. (2010) Characterization of EMU, the Arabidopsis homolog of the yeast THO complex member HPR1. *RNA*, **16**, 1809–1817.
- Gewartowski, K., Cuellar, J., Dziembowski, A. and Valpuesta, J.M. (2012) The yeast THO complex forms a 5-subunit assembly that directly interacts with active chromatin. *Bioarchitecture*, **2**, 134–137.
- Han, M.H., Goud, S., Song, L. and Fedoroff, N. (2004) The Arabidopsis double-stranded RNA-binding protein HYL1 plays a role in microRNA-mediated gene regulation. *Proc. Natl Acad. Sci. USA*, **101**, 1093–1098.
- Hugouvieux, V., Kwak, J.M. and Schroeder, J.I. (2001) An mRNA cap binding protein, ABH1, modulates early abscisic acid signal transduction in *Arabidopsis*. *Cell*, **106**, 477–487.
- Jauvin, V., Elmayer, T. and Vaucheret, H. (2010) The conserved RNA trafficking proteins HPR1 and TEX1 are involved in the production of endogenous and exogenous small interfering RNA in *Arabidopsis*. *Plant Cell*, **22**, 2697–2709.
- Jones-Rhoades, M.W., Bartel, D.P. and Bartel, B. (2006) MicroRNAs and their regulatory roles in plants. *Annu. Rev. Plant Biol.* **57**, 19–53.
- Kim, S., Yang, J.Y., Xu, J., Jang, I.C., Prigge, M.J. and Chua, N.H. (2008) Two cap-binding proteins CBP20 and CBP80 are involved in processing primary microRNAs. *Plant Cell Physiol.* **49**, 1634–1644.
- Laubinger, S., Sachsenberg, T., Zeller, G., Busch, W., Lohmann, J.U., Ratsch, G. and Weigel, D. (2008) Dual roles of the nuclear cap-binding complex and SERRATE in pre-mRNA splicing and microRNA processing in *Arabidopsis thaliana*. *Proc. Natl Acad. Sci. USA*, **105**, 8795–8800.
- Liu, Y.G., Mitsukawa, N., Oosumi, T. and Whittier, R.F. (1995) Efficient isolation and mapping of Arabidopsis thaliana T-DNA insert junctions by thermal asymmetric interlaced PCR. *Plant J.* **8**, 457–463.
- Lorkovic, Z.J., Hilscher, J. and Barta, A. (2004) Use of fluorescent protein tags to study nuclear organization of the spliceosomal machinery in transiently transformed living plant cells. *Mol. Biol. Cell*, **15**, 3233–3243.
- Manavella, P.A., Hagmann, J., Ott, F., Laubinger, S., Franz, M., Macek, B. and Weigel, D. (2012a) Fast-forward genetics identifies plant CPL phosphatases as regulators of miRNA processing factor HYL1. *Cell*, **151**, 859–870.
- Manavella, P.A., Koenig, D. and Weigel, D. (2012b) Plant secondary siRNA production determined by microRNA-duplex structure. *Proc. Natl Acad. Sci. USA*, **109**, 2461–2466.
- Manavella, P.A., Koenig, D., Rubio-Somoza, I., Burbano, H.A., Becker, C. and Weigel, D. (2013) Tissue-specific silencing of Arabidopsis SU(VAR)3-9 HOMOLOG8 by miR171a. *Plant Physiol.* **161**, 805–812.
- Masuda, S., Das, R., Cheng, H., Hurt, E., Dorman, N. and Reed, R. (2005) Recruitment of the human TREX complex to mRNA during splicing. *Genes Dev.* **19**, 1512–1517.
- Mathieu, J., Warthmann, N., Kuttner, F. and Schmid, M. (2007) Export of FT protein from phloem companion cells is sufficient for floral induction in *Arabidopsis*. *Curr. Biol.* **17**, 1055–1060.
- Moon, S., Cho, B., Min, S.H., Lee, D. and Chung, Y.D. (2011) The THO complex is required for nucleolar integrity in *Drosophila* spermatocytes. *Development*, **138**, 3835–3845.
- Murray, M.G. and Thompson, W.F. (1980) Rapid isolation of high molecular weight plant DNA. *Nucleic Acids Res.* **8**, 4321–4325.
- Papp, I., Mur, L.A., Dalmadi, A., Dulai, S. and Koncz, C. (2004) A mutation in the Cap Binding Protein 20 gene confers drought tolerance to *Arabidopsis*. *Plant Mol. Biol.* **55**, 679–686.
- Pena, A., Gewartowski, K., Mroczek, S. et al. (2012) Architecture and nucleic acids recognition mechanism of the THO complex, an mRNP assembly factor. *EMBO J.* **31**, 1605–1616.

- Piruat, J.I. and Aguilera, A.** (1998) A novel yeast gene, THO2, is involved in RNA pol II transcription and provides new evidence for transcriptional elongation-associated recombination. *EMBO J.* **17**, 4859–4872.
- Rappsilber, J., Ryder, U., Lamond, A.I. and Mann, M.** (2002) Large-scale proteomic analysis of the human spliceosome. *Genome Res.* **12**, 1231–1245.
- Reed, R. and Cheng, H.** (2005) TREX, SR proteins and export of mRNA. *Curr. Opin. Cell Biol.* **17**, 269–273.
- Ren, G., Xie, M., Dou, Y., Zhang, S., Zhang, C. and Yu, B.** (2012) Regulation of miRNA abundance by RNA binding protein TOUGH in Arabidopsis. *Proc. Natl Acad. Sci. USA*, **109**, 12817–12821.
- Smith, L.M., Pontes, O., Searle, I., Yelina, N., Yousafzai, F.K., Herr, A.J., Pikaard, C.S. and Baulcombe, D.C.** (2007) An SNF2 protein associated with nuclear RNA silencing and the spread of a silencing signal between cells in Arabidopsis. *Plant Cell*, **19**, 1507–1521.
- Song, L., Han, M.H., Lesicka, J. and Fedoroff, N.** (2007) Arabidopsis primary microRNA processing proteins HYL1 and DCL1 define a nuclear body distinct from the Cajal body. *Proc. Natl Acad. Sci. USA*, **104**, 5437–5442.
- Terzi, L.C. and Simpson, G.G.** (2009) Arabidopsis RNA immunoprecipitation. *Plant J.* **59**, 163–168.
- Voinnet, O.** (2009) Origin, biogenesis, and activity of plant microRNAs. *Cell*, **136**, 669–687.
- Weigel, D., Ahn, J.H., Blazquez, M.A. et al.** (2000) Activation tagging in Arabidopsis. *Plant Physiol.* **122**, 1003–1013.
- Wu, X., Shi, Y., Li, J., Xu, L., Fang, Y., Li, X. and Qi, Y.** (2013) A role for the RNA-binding protein MOS2 in microRNA maturation in Arabidopsis. *Cell Res.* **23**, 645–657.
- Yelina, N.E., Smith, L.M., Jones, A.M., Patel, K., Kelly, K.A. and Baulcombe, D.C.** (2010) Putative Arabidopsis THO/TREX mRNA export complex is involved in transgene and endogenous siRNA biosynthesis. *Proc. Natl Acad. Sci. USA*, **107**, 13948–13953.
- Yu, B., Bi, L., Zheng, B. et al.** (2008) The FHA domain proteins DAWDLE in Arabidopsis and SNIP1 in humans act in small RNA biogenesis. *Proc. Natl Acad. Sci. USA*, **105**, 10073–10078.